EUROPEAN ORGANIZATION FOR NUCLEAR RESEARCH

CERN-EP/2002-034
May 15, 2002

The $e^+e^- \rightarrow Z\gamma\gamma \rightarrow q\bar{q}\gamma\gamma$ Reaction at LEP and Constraints on Anomalous Quartic Gauge Boson Couplings

The L3 Collaboration

Abstract

The cross section of the process $e^+e^- \rightarrow Z\gamma\gamma \rightarrow q\bar{q}\gamma\gamma$ is measured with $215\,\mathrm{pb}^{-1}$ of data collected with the L3 detector during the final LEP run at centre-of-mass energies around 205 GeV and 207 GeV. No deviation from the Standard Model expectation is observed. The full data sample of $713\,\mathrm{pb}^{-1}$, collected above the Z resonance, is used to constrain the coefficients of anomalous quartic gauge boson couplings to:

$$-0.02\ \mathrm{GeV}^{-2} < \quad a_0/\Lambda^2 \quad < 0.03\ \mathrm{GeV}^{-2} \text{ and}$$
$$-0.07\ \mathrm{GeV}^{-2} < \quad a_c/\Lambda^2 \quad < 0.05\ \mathrm{GeV}^{-2},$$

at 95% confidence level.

Submitted to *Phys. Lett. B*

Introduction

High energy e^+e^- collisions offer a unique environment to unveil the structure of the couplings between gauge bosons. Extensive studies of boson pair-production are performed to probe triple vertices of neutral and charged bosons. Results were recently reported on the investigation of triple boson production through the reactions $e^+e^- \to W^+W^-\gamma$ [1,2] and $e^+e^- \to Z\gamma\gamma$ [3,4]. These processes give access to possible anomalous Quartic Gauge boson Couplings (QGCs).

Figures 1a–c display three of the six Standard Model diagrams that describe the $e^+e^- \to Z\gamma\gamma$ process with the radiation of photons from the incoming electrons. This process is studied exploiting the high branching fraction of the Z boson decay into hadrons. The $e^+e^- \to Z\gamma\gamma \to q\bar{q}\gamma\gamma$ signal is defined [4] by phase-space requirements on the energies E_γ and angles θ_γ of the two photons, on the propagator mass $\sqrt{s'}$ and on the angle $\theta_{\gamma q}$ between each photon and the nearest quark:

$$E_\gamma > 5\ \mathrm{GeV}, \quad |\cos\theta_\gamma| < 0.97, \quad |\sqrt{s'} - m_Z| < 2\Gamma_Z, \ \text{ and } \ \cos\theta_{\gamma q} < 0.98, \tag{1}$$

where m_Z and Γ_Z are the Z boson mass and width. Events with hadrons and initial state photons falling outside the signal definition cuts are referred to as "non-resonant" background.

A single initial state radiation photon can also lower the effective centre-of-mass energy of the e^+e^- collision to around m_Z. This photon can be mistaken for the most energetic photon of the signal and two sources can then mimic the least energetic photon: the direct radiation of photons from the quarks, or photons originating from hadronic decays, misidentified electrons or unresolved π^0's. These background processes are depicted in Figures 1d and 1e, respectively.

In the Standard Model, the $Z\gamma\gamma$ production via QGCs is forbidden at tree level. Possible contributions of anomalous QGCs, through the diagram sketched in Figure 1f, are described by two terms of dimension-six in an effective Lagrangian [5,6]:

$$\begin{aligned} \mathcal{L}_6^0 &= -\frac{\pi\alpha}{4\Lambda^2} a_0 F_{\mu\nu} F^{\mu\nu} \vec{W}_\rho \cdot \vec{W}^\rho \\ \mathcal{L}_6^c &= -\frac{\pi\alpha}{4\Lambda^2} a_c F_{\mu\rho} F^{\mu\sigma} \vec{W}^\rho \cdot \vec{W}_\sigma, \end{aligned}$$

where α is the fine structure constant, $F_{\mu\nu}$ is the photon field and $\vec{W}_\sigma$ is the weak boson field. The parameters a_0 and a_c describe the strength of the QGCs and Λ represents the scale of the New Physics responsible for these anomalous contributions. In the Standard Model, $a_0 = a_c = 0$. Experimental limits on QGCs were derived from studies of the $e^+e^- \to W^+W^-\gamma$ process [1,2]. However, the a_0 and a_c couplings might be different in the $e^+e^- \to Z\gamma\gamma$ case. Alternative parametrisations can be found in References 7 and 8. Indirect bounds on QGCs were extracted in Reference 9 using Z pole data.

Data Analysis

Reference 4 describes the analysis of the $e^+e^- \to Z\gamma\gamma \to q\bar{q}\gamma\gamma$ process with $497.6\,\mathrm{pb}^{-1}$ of data collected by the L3 detector [10] at LEP at centre-of-mass energies, $\sqrt{s}$, between 130 and 202 GeV. This Letter details the equivalent findings from the final LEP run, when the machine was operated at $\sqrt{s} = 200 - 209$ GeV. These data are grouped in two energy bins around average $\sqrt{s}$ values of 204.8 GeV and 206.6 GeV, respectively corresponding to integrated luminosities of $77.4\,\mathrm{pb}^{-1}$ and $137.9\,\mathrm{pb}^{-1}$.

The signal and the "non-resonant" background are described with the KK2f Monte Carlo program [11], which takes into account the interference of diagrams with initial and final state photons. It is interfaced with the JETSET [12] program for the simulation of hadronisation.

Other backgrounds are generated with the Monte Carlo programs PYTHIA [12] ($e^+e^- \rightarrow Ze^+e^-$ and $e^+e^- \rightarrow ZZ$), KORALZ [13] ($e^+e^- \rightarrow \tau^+\tau^-(\gamma)$), PHOJET [14] ($e^+e^- \rightarrow e^+e^-$ hadrons) and KORALW [15] for W^+W^- production except for the $e\nu_e q\bar{q}'$ final states, generated with EXCALIBUR [16]. The L3 detector response is simulated using the GEANT [17] and GHEISHA [18] programs, which model the effects of energy loss, multiple scattering and showering in the detector. Time dependent detector inefficiencies, as monitored during data taking periods, are also simulated

Candidates for the $e^+e^- \rightarrow Z\gamma\gamma \rightarrow q\bar{q}\gamma\gamma$ process are longitudinally and transversely balanced hadronic events with two isolated photons with reconstructed energy above 5 GeV, detected in a polar angle range $|\cos\theta| < 0.97$. The invariant mass of the reconstructed hadronic system, $M_{q\bar{q}}$, is required to be consistent with m_Z: 74 GeV $< M_{q\bar{q}} <$ 111 GeV.

The main background after these requirements is due to the "non-resonant" production of two photons and a hadronic system. The relativistic velocity $\beta_Z = p_Z/E_Z$ of the Z candidate is calculated from the kinematics of the observed photons, assuming its mass to be m_Z. As shown in Figure 2a, β_Z is larger for part of these background events than for the signal. Requiring $\beta_Z < 0.73$ rejects half of this background.

Events with a single initial state radiation photon, such as those shown in Figure 1d and Figure 1e, are rejected by an upper bound on the energy $E_{\gamma 1}$ of the most energetic photon. This cut is chosen as $E_{\gamma 1} < 79.9$ GeV at $\sqrt{s} = 204.8$ GeV and $E_{\gamma 1} < 80.6$ GeV at $\sqrt{s} = 205.6$ GeV. A lower bound of 17° on the angle ω between the direction of the least energetic photon and that of the closest jet is also imposed. Data and Monte Carlo distributions of these selection variables are presented in Figure 2. Good agreement is observed.

Table 1 lists the signal efficiencies and the numbers of events selected in the data and Monte Carlo samples. A signal purity around 75% is obtained. The dominant background consists of hadronic events with photons. Half of these are "non-resonant" events, the other half being events with final state radiation or fake photons.

Cross Section Measurement

A clear Z signal is observed in the spectrum of the recoil mass to the two photons, as presented in Figure 3a. The $e^+e^- \rightarrow Z\gamma\gamma \rightarrow q\bar{q}\gamma\gamma$ cross section, σ, is determined in the kinematical region defined by Equation (1) at each average $\sqrt{s}$ by a fit to the recoil mass spectrum. The background predictions and the signal shape are fixed, while the signal normalisation is fitted. The results are[1)]:

$$\begin{array}{lcll} \sigma(204.8\ \text{GeV}) & = & 0.30^{+0.11}_{-0.09} \pm 0.03\,\text{pb} & (\sigma_{\text{SM}} = 0.287 \pm 0.003\,\text{pb}) \\ \sigma(206.6\ \text{GeV}) & = & 0.25^{+0.07}_{-0.06} \pm 0.03\,\text{pb} & (\sigma_{\text{SM}} = 0.281 \pm 0.003\,\text{pb}). \end{array}$$

Here and below, the first quoted uncertainties are statistical and the second ones systematic. The systematic uncertainties on the cross section measurement are of the order of 10% [4], mainly due to the limited Monte Carlo statistics and the uncertainty on the energy scale of the detector.

[1)] The cross section is also measured in the more restrictive phase space defined by tightening the bounds on θ_γ and $\theta_{\gamma q}$ to $|\cos\theta_\gamma| < 0.95$ and $\cos\theta_{\gamma q} < 0.9$. For the full 215 pb^{-1} at the combined average $\sqrt{s}$ of 205.9 GeV, the result is: $\sigma(205.9\ \text{GeV}) = 0.18 \pm 0.06 \pm 0.02\,\text{pb}$, with a Standard Model expectation of $\sigma_{SM} = 0.172 \pm 0.003\,\text{pb}$.

The measurements are in good agreement with the theoretical predictions, σ_{SM}, as calculated with the KK2f Monte Carlo program. The uncertainty on the predictions (1.5%) is the quadratic sum of the theory uncertainty [11] and the statistical uncertainty of the Monte Carlo sample used for the calculation. These results and those obtained at lower centre-of-mass energies [4] are compared in Figure 4 to the expected Standard Model cross section as a function of $\sqrt{s}$.

Figure 3b shows the recoil mass spectrum for the total data sample of 712.9 pb^{-1} collected at LEP above the Z resonance, comprising the data discussed in this Letter and those at lower centre-of-mass energies [4]. A fit to this spectrum determines the ratio $R_{\mathrm{Z}\gamma\gamma}$ between all the observed data and the signal expectations as:

$$R_{\mathrm{Z}\gamma\gamma} = \frac{\sigma}{\sigma_{\mathrm{SM}}} = 0.86 \pm 0.09 \pm 0.06,$$

in agreement with the Standard Model. The correlation of systematic uncertainties between the different data samples amounts to 50% and is taken into account in the fit.

$\sqrt{s}$(GeV)	ε(%)	Data	Monte Carlo	N_s	$N_b^{\mathrm{q\bar{q}}}$	N_b^{Other}
204.8	51	17	14.7 ± 0.5	11.3 ± 0.5	3.09 ± 0.02	0.31 ± 0.03
206.6	50	23	24.7 ± 0.5	19.5 ± 0.5	4.53 ± 0.04	0.67 ± 0.03

Table 1: Results of the $\mathrm{e^+e^-} \rightarrow \mathrm{Z}\gamma\gamma \rightarrow \mathrm{q\bar{q}}\gamma\gamma$ selection. The signal efficiencies, ε, are given, together with the observed and expected numbers of events. Expectations for signal, N_s, hadronic processes with photons, $N_b^{\mathrm{q\bar{q}}}$, and other backgrounds, N_b^{Other}, are listed. Uncertainties are due to Monte Carlo statistics.

Constraints on Quartic Gauge Boson Couplings

Anomalous values of QGCs would manifest themselves as deviations in the total $\mathrm{e^+e^-} \rightarrow \mathrm{Z}\gamma\gamma$ cross section as a function of $\sqrt{s}$, as presented in Figure 4. A harder energy spectrum for the least energetic photon [6] constitutes a further powerful experimental signature, as shown in Figure 5 for the full data sample collected at $\sqrt{s} = 130 - 209$ GeV. QGC predictions for the cross section and this spectrum are obtained by reweighting the Standard Model signal Monte Carlo events. A modified version of the WRAP [19] Monte Carlo program, that includes the QGC matrix element, is used.

The energy spectra of the least energetic photon are fitted for the two $\sqrt{s}$ values discussed in this Letter and the eight values of $\sqrt{s}$ of Reference 4. Each of the two parameters describing the QGCs is left free in turn, the other being fixed to zero. The fits yield the 68% confidence level results:

$$a_0/\Lambda^2 = 0.00^{+0.02}_{-0.01}\ \mathrm{GeV}^{-2} \ \text{ and } \ a_c/\Lambda^2 = 0.03^{+0.01}_{-0.02}\ \mathrm{GeV}^{-2},$$

in agreement with the expected Standard Model values of zero. A simultaneous fit to both parameters yields the 95% confidence level limits:

$$-0.02\ \mathrm{GeV}^{-2} < a_0/\Lambda^2 < 0.03\ \mathrm{GeV}^{-2} \ \text{ and } \ -0.07\ \mathrm{GeV}^{-2} < a_c/\Lambda^2 < 0.05\ \mathrm{GeV}^{-2},$$

as shown in Figure 6. A correlation coefficient of -16% is observed. Experimental systematic uncertainties as well as those on the Standard Model $\mathrm{e^+e^-} \rightarrow \mathrm{Z}\gamma\gamma \rightarrow \mathrm{q\bar{q}}\gamma\gamma$ cross section predictions are taken into account in the fit. These results supersede those previously obtained at lower $\sqrt{s}$ [4], as they are based on the full data sample and an improved modelling of QGC effects.

In conclusion, the $e^+e^- \rightarrow Z\gamma\gamma \rightarrow q\bar{q}\gamma\gamma$ process is found to be well described by the Standard Model predictions [11], with no evidence for anomalous values of QGCs.

References

[1] OPAL Collab., G. Abbiendi *et al.*, Phys. Lett. **B 471** (1999) 293.

[2] L3 Collab., M. Acciarri *et al.*, Phys. Lett. **B 490** (2000) 187; L3 Collab., M. Acciarri *et al.*, Phys. Lett. **B 527** (2002) 29.

[3] L3 Collab., M. Acciarri *et al.*, Phys. Lett. **B 478** (2000) 39.

[4] L3 Collab., M. Acciarri *et al.*, Phys. Lett. **B 505** (2001) 47.

[5] G. Bélanger and F. Boudjema, Phys. Lett. **B 288** (1992) 201.

[6] W. J. Stirling and A. Werthenbach, Eur. Phys. J. **C 14** (2000) 103.

[7] G. Bélanger *et al.*, Eur. Phys. J. **C 13** (2000) 283.

[8] A. Denner *et al.*, Eur. Phys. J. **C 20** (2001).

[9] A. Brunstein, O. J. P. Éboli and M. C. Gonzales-Garcia, Phys. Lett. **B 375** (1996) 233.

[10] L3 Collab., B. Adeva *et al.*, Nucl. Instr. and Meth. **A 289** (1990) 35; L3 Collab., O. Adriani *et al.*, Phys. Rep. **236** (1993) 1; I. C. Brock *et al.*, Nucl. Instr. and Meth. **A 381** (1996) 236; M. Chemarin *et al.*, Nucl. Instr. and Meth. **A 349** (1994) 345; M. Acciarri *et al.*, Nucl. Instr. and Meth. **A 351** (1994) 300; A. Adam *et al.*, Nucl. Instr. and Meth. **A 383** (1996) 342; G. Basti *et al.*, Nucl. Instr. and Meth. **A 374** (1996) 293.

[11] KK2f version 4.13 is used; S. Jadach, B.F.L. Ward and Z. Wąs, Comp. Phys. Comm **130** (2000) 260.

[12] PYTHIA version 5.772 and JETSET version 7.4 are used; T. Sjöstrand, Preprint CERN–TH/7112/93 (1993), revised 1995; T. Sjöstrand, Comp. Phys. Comm. **82** (1994) 74.

[13] KORALZ version 4.03 is used; S. Jadach, B. F. L. Ward and Z. Wąs, Comp. Phys. Comm **79** (1994) 503.

[14] PHOJET version 1.05 is used; R. Engel, Z. Phys. **C 66** (1995) 203; R. Engel and J. Ranft, Phys. Rev. **D 54** (1996) 4244.

[15] KORALW version 1.33 is used; M. Skrzypek *et al.*, Comp. Phys. Comm. **94** (1996) 216; M. Skrzypek *et al.*, Phys. Lett. **B 372** (1996) 289.

[16] R. Kleiss and R. Pittau, Comp. Phys. Comm. **85** (1995) 447; R. Pittau, Phys. Lett. **B 335** (1994) 490.

[17] GEANT version 3.15 is used; R. Brun *et al.*, preprint CERN–DD/EE/84–1 (1984), revised 1987.

[18] H. Fesefeldt, report RWTH Aachen PITHA 85/02 (1985).

[19] G. Montagna *et al.*, Phys. Lett. **B 515** (2001) 197. We are indebited to G. Montagna, M. Moretti, O. Nicrosini, M. Osmo and F.Piccinini for having provided us with the WRAP reweighting function.

The L3 Collaboration:

P.Achard,[21] O.Adriani,[18] M.Aguilar-Benitez,[25] J.Alcaraz,[25,19] G.Alemanni,[23] J.Allaby,[19] A.Aloisio,[29] M.G.Alviggi,[29] H.Anderhub,[47] V.P.Andreev,[6,34] F.Anselmo,[9] A.Arefiev,[28] T.Azemoon,[3] T.Aziz,[10,19] P.Bagnaia,[39] A.Bajo,[25] G.Baksay,[26] L.Baksay,[26] S.V.Baldew,[2] S.Banerjee,[10] Sw.Banerjee,[4] A.Barczyk,[47,45] R.Barillère,[19] P.Bartalini,[23] M.Basile,[9] N.Batalova,[44] R.Battiston,[33] A.Bay,[23] F.Becattini,[18] U.Becker,[14] F.Behner,[47] L.Bellucci,[18] R.Berbeco,[3] J.Berdugo,[25] P.Berges,[14] B.Bertucci,[33] B.L.Betev,[47] M.Biasini,[33] M.Biglietti,[29] A.Biland,[47] J.J.Blaising,[4] S.C.Blyth,[35] G.J.Bobbink,[2] A.Böhm,[1] L.Boldizsar,[13] B.Borgia,[39] S.Bottai,[18] D.Bourilkov,[47] M.Bourquin,[21] S.Braccini,[21] J.G.Branson,[41] F.Brochu,[4] J.D.Burger,[14] W.J.Burger,[33] X.D.Cai,[14] M.Capell,[14] G.Cara Romeo,[9] G.Carlino,[29] A.Cartacci,[18] J.Casaus,[25] F.Cavallari,[39] N.Cavallo,[36] C.Cecchi,[33] M.Cerrada,[25] M.Chamizo,[21] Y.H.Chang,[49] M.Chemarin,[24] A.Chen,[49] G.Chen,[7] G.M.Chen,[7] H.F.Chen,[22] H.S.Chen,[7] G.Chiefari,[29] L.Cifarelli,[40] F.Cindolo,[9] I.Clare,[14] R.Clare,[38] G.Coignet,[4] N.Colino,[25] S.Costantini,[39] B.de la Cruz,[25] S.Cucciarelli,[33] J.A.van Dalen,[31] R.de Asmundis,[29] P.Déglon,[21] J.Debreczeni,[13] A.Degré,[4] K.Dehmelt,[26] K.Deiters,[45] D.della Volpe,[29] E.Delmeire,[21] P.Denes,[37] F.DeNotaristefani,[39] A.De Salvo,[47] M.Diemoz,[39] M.Dierckxsens,[2] C.Dionisi,[39] M.Dittmar,[47,19] A.Doria,[29] M.T.Dova,[11,♯] D.Duchesneau,[4] B.Echenard,[21] A.Eline,[19] H.El Mamouni,[24] A.Engler,[35] F.J.Eppling,[14] A.Ewers,[1] P.Extermann,[21] M.A.Falagan,[25] S.Falciano,[39] A.Favara,[32] J.Fay,[24] O.Fedin,[34] M.Felcini,[47] T.Ferguson,[35] H.Fesefeldt,[1] E.Fiandrini,[33] J.H.Field,[21] F.Filthaut,[31] P.H.Fisher,[14] W.Fisher,[37] I.Fisk,[41] G.Forconi,[14] K.Freudenreich,[47] C.Furetta,[27] Yu.Galaktionov,[28,14] S.N.Ganguli,[10] P.Garcia-Abia,[5,19] M.Gataullin,[32] S.Gentile,[39] S.Giagu,[39] Z.F.Gong,[22] G.Grenier,[24] O.Grimm,[47] M.W.Gruenewald,[17] M.Guida,[40] R.van Gulik,[2] V.K.Gupta,[37] A.Gurtu,[10] L.J.Gutay,[44] D.Haas,[5] R.Sh.Hakobyan,[31] D.Hatzifotiadou,[9] T.Hebbeker,[1] A.Hervé,[19] J.Hirschfelder,[35] H.Hofer,[47] M.Hohlmann,[26] G.Holzner,[47] S.R.Hou,[49] Y.Hu,[31] B.N.Jin,[7] L.W.Jones,[3] P.de Jong,[2] I.Josa-Mutuberría,[25] D.Käfer,[1] M.Kaur,[15] M.N.Kienzle-Focacci,[21] J.K.Kim,[43] J.Kirkby,[19] W.Kittel,[31] A.Klimentov,[14,28] A.C.König,[31] M.Kopal,[44] V.Koutsenko,[14,28] M.Kräber,[47] R.W.Kraemer,[35] W.Krenz,[1] A.Krüger,[46] A.Kunin,[14] P.Ladron de Guevara,[25] I.Laktineh,[24] G.Landi,[18] J.Lätt,[21] M.Lebeau,[19] A.Lebedev,[14] P.Lebrun,[24] P.Lecomte,[47] P.Lecoq,[19] P.Le Coultre,[47] J.M.Le Goff,[19] R.Leiste,[46] M.Levtchenko,[27] P.Levtchenko,[34] C.Li,[22] S.Likhoded,[46] C.H.Lin,[49] W.T.Lin,[49] F.L.Linde,[2] L.Lista,[29] Z.A.Liu,[7] W.Lohmann,[46] E.Longo,[39] Y.S.Lu,[7] K.Lübelsmeyer,[1] C.Luci,[39] L.Luminari,[39] W.Lustermann,[47] W.G.Ma,[22] L.Malgeri,[21] A.Malinin,[28] C.Maña,[25] D.Mangeol,[31] J.Mans,[37] J.P.Martin,[24] F.Marzano,[39] K.Mazumdar,[10] R.R.McNeil,[6] S.Mele,[19,29] L.Merola,[29] M.Meschini,[18] W.J.Metzger,[31] A.Mihul,[12] H.Milcent,[19] G.Mirabelli,[39] J.Mnich,[1] G.B.Mohanty,[10] G.S.Muanza,[24] A.J.M.Muijs,[2] B.Musicar,[41] M.Musy,[39] S.Nagy,[16] S.Natale,[21] M.Napolitano,[29] F.Nessi-Tedaldi,[47] H.Newman,[32] T.Niessen,[1] A.Nisati,[39] H.Nowak,[46] R.Ofierzynski,[47] G.Organtini,[39] C.Palomares,[19] D.Pandoulas,[1] P.Paolucci,[29] R.Paramatti,[39] G.Passaleva,[18] S.Patricelli,[29] T.Paul,[11] M.Pauluzzi,[33] C.Paus,[14] F.Pauss,[47] M.Pedace,[39] S.Pensotti,[27] D.Perret-Gallix,[4] B.Petersen,[31] D.Piccolo,[29] F.Pierella,[9] M.Pioppi,[33] P.A.Piroué,[37] E.Pistolesi,[27] V.Plyaskin,[28] M.Pohl,[21] V.Pojidaev,[18] J.Pothier,[19] D.O.Prokofiev,[44] D.Prokofiev,[34] J.Quartieri,[40] G.Rahal-Callot,[47] M.A.Rahaman,[10] P.Raics,[16] N.Raja,[10] R.Ramelli,[47] P.G.Rancoita,[27] R.Ranieri,[18] A.Raspereza,[46] P.Razis,[30] D.Ren,[47] M.Rescigno,[39] S.Reucroft,[11] S.Riemann,[46] K.Riles,[3] B.P.Roe,[3] L.Romero,[25] A.Rosca,[8] S.Rosier-Lees,[4] S.Roth,[1] C.Rosenbleck,[1] B.Roux,[31] J.A.Rubio,[19] G.Ruggiero,[18] H.Rykaczewski,[47] A.Sakharov,[47] S.Saremi,[6] S.Sarkar,[39] J.Salicio,[19] E.Sanchez,[25] M.P.Sanders,[31] C.Schäfer,[19] V.Schegelsky,[34] S.Schmidt-Kaerst,[1] D.Schmitz,[1] H.Schopper,[48] D.J.Schotanus,[31] G.Schwering,[1] C.Sciacca,[29] L.Servoli,[33] S.Shevchenko,[32] N.Shivarov,[42] V.Shoutko,[14] E.Shumilov,[28] A.Shvorob,[32] T.Siedenburg,[1] D.Son,[43] C.Souga,[24] P.Spillantini,[18] M.Steuer,[14] D.P.Stickland,[37] B.Stoyanov,[42] A.Straessner,[19] K.Sudhakar,[10] G.Sultanov,[42] L.Z.Sun,[22] S.Sushkov,[8] H.Suter,[47] J.D.Swain,[11] Z.Szillasi,[26,¶] X.W.Tang,[7] P.Tarjan,[16] L.Tauscher,[5] L.Taylor,[11] B.Tellili,[24] D.Teyssier,[24] C.Timmermans,[31] Samuel C.C.Ting,[14] S.M.Ting,[14] S.C.Tonwar,[10,19] J.Tóth,[13] C.Tully,[37] K.L.Tung,[7] J.Ulbricht,[47] E.Valente,[39] R.T.Van de Walle,[31] R.Vasquez,[44] V.Veszpremi,[26] G.Vesztergombi,[13] I.Vetlitsky,[28] D.Vicinanza,[40] G.Viertel,[47] S.Villa,[38] M.Vivargent,[4] S.Vlachos,[5] I.Vodopianov,[34] H.Vogel,[35] H.Vogt,[46] I.Vorobiev,[35,28] A.A.Vorobyov,[34] M.Wadhwa,[5] W.Wallraff,[1] X.L.Wang,[22] Z.M.Wang,[22] M.Weber,[1] P.Wienemann,[1] H.Wilkens,[31] S.Wynhoff,[37] L.Xia,[32] Z.Z.Xu,[22] J.Yamamoto,[3] B.Z.Yang,[22] C.G.Yang,[7] H.J.Yang,[3] M.Yang,[7] S.C.Yeh,[50] An.Zalite,[34] Yu.Zalite,[34] Z.P.Zhang,[22] J.Zhao,[22] G.Y.Zhu,[7] R.Y.Zhu,[32] H.L.Zhuang,[7] A.Zichichi,[9,19,20] B.Zimmermann,[47] M.Zöller.[1]

1 I. Physikalisches Institut, RWTH, D-52056 Aachen, FRG[§]
III. Physikalisches Institut, RWTH, D-52056 Aachen, FRG[§]
2 National Institute for High Energy Physics, NIKHEF, and University of Amsterdam, NL-1009 DB Amsterdam, The Netherlands
3 University of Michigan, Ann Arbor, MI 48109, USA
4 Laboratoire d'Annecy-le-Vieux de Physique des Particules, LAPP,IN2P3-CNRS, BP 110, F-74941 Annecy-le-Vieux CEDEX, France
5 Institute of Physics, University of Basel, CH-4056 Basel, Switzerland
6 Louisiana State University, Baton Rouge, LA 70803, USA
7 Institute of High Energy Physics, IHEP, 100039 Beijing, China[△]
8 Humboldt University, D-10099 Berlin, FRG[§]
9 University of Bologna and INFN-Sezione di Bologna, I-40126 Bologna, Italy
10 Tata Institute of Fundamental Research, Mumbai (Bombay) 400 005, India
11 Northeastern University, Boston, MA 02115, USA
12 Institute of Atomic Physics and University of Bucharest, R-76900 Bucharest, Romania
13 Central Research Institute for Physics of the Hungarian Academy of Sciences, H-1525 Budapest 114, Hungary[‡]
14 Massachusetts Institute of Technology, Cambridge, MA 02139, USA
15 Panjab University, Chandigarh 160 014, India.
16 KLTE-ATOMKI, H-4010 Debrecen, Hungary[¶]
17 Department of Experimental Physics, University College Dublin, Belfield, Dublin 4, Ireland
18 INFN Sezione di Firenze and University of Florence, I-50125 Florence, Italy
19 European Laboratory for Particle Physics, CERN, CH-1211 Geneva 23, Switzerland
20 World Laboratory, FBLJA Project, CH-1211 Geneva 23, Switzerland
21 University of Geneva, CH-1211 Geneva 4, Switzerland
22 Chinese University of Science and Technology, USTC, Hefei, Anhui 230 029, China[△]
23 University of Lausanne, CH-1015 Lausanne, Switzerland
24 Institut de Physique Nucléaire de Lyon, IN2P3-CNRS,Université Claude Bernard, F-69622 Villeurbanne, France
25 Centro de Investigaciones Energéticas, Medioambientales y Tecnológicas, CIEMAT, E-28040 Madrid, Spain♭
26 Florida Institute of Technology, Melbourne, FL 32901, USA
27 INFN-Sezione di Milano, I-20133 Milan, Italy
28 Institute of Theoretical and Experimental Physics, ITEP, Moscow, Russia
29 INFN-Sezione di Napoli and University of Naples, I-80125 Naples, Italy
30 Department of Physics, University of Cyprus, Nicosia, Cyprus
31 University of Nijmegen and NIKHEF, NL-6525 ED Nijmegen, The Netherlands
32 California Institute of Technology, Pasadena, CA 91125, USA
33 INFN-Sezione di Perugia and Università Degli Studi di Perugia, I-06100 Perugia, Italy
34 Nuclear Physics Institute, St. Petersburg, Russia
35 Carnegie Mellon University, Pittsburgh, PA 15213, USA
36 INFN-Sezione di Napoli and University of Potenza, I-85100 Potenza, Italy
37 Princeton University, Princeton, NJ 08544, USA
38 University of Californa, Riverside, CA 92521, USA
39 INFN-Sezione di Roma and University of Rome, "La Sapienza", I-00185 Rome, Italy
40 University and INFN, Salerno, I-84100 Salerno, Italy
41 University of California, San Diego, CA 92093, USA
42 Bulgarian Academy of Sciences, Central Lab. of Mechatronics and Instrumentation, BU-1113 Sofia, Bulgaria
43 The Center for High Energy Physics, Kyungpook National University, 702-701 Taegu, Republic of Korea
44 Purdue University, West Lafayette, IN 47907, USA
45 Paul Scherrer Institut, PSI, CH-5232 Villigen, Switzerland
46 DESY, D-15738 Zeuthen, FRG
47 Eidgenössische Technische Hochschule, ETH Zürich, CH-8093 Zürich, Switzerland
48 University of Hamburg, D-22761 Hamburg, FRG
49 National Central University, Chung-Li, Taiwan, China
50 Department of Physics, National Tsing Hua University, Taiwan, China
§ Supported by the German Bundesministerium für Bildung, Wissenschaft, Forschung und Technologie
‡ Supported by the Hungarian OTKA fund under contract numbers T019181, F023259 and T037350.
¶ Also supported by the Hungarian OTKA fund under contract number T026178.
♭ Supported also by the Comisión Interministerial de Ciencia y Tecnología.
♯ Also supported by CONICET and Universidad Nacional de La Plata, CC 67, 1900 La Plata, Argentina.
△ Supported by the National Natural Science Foundation of China.

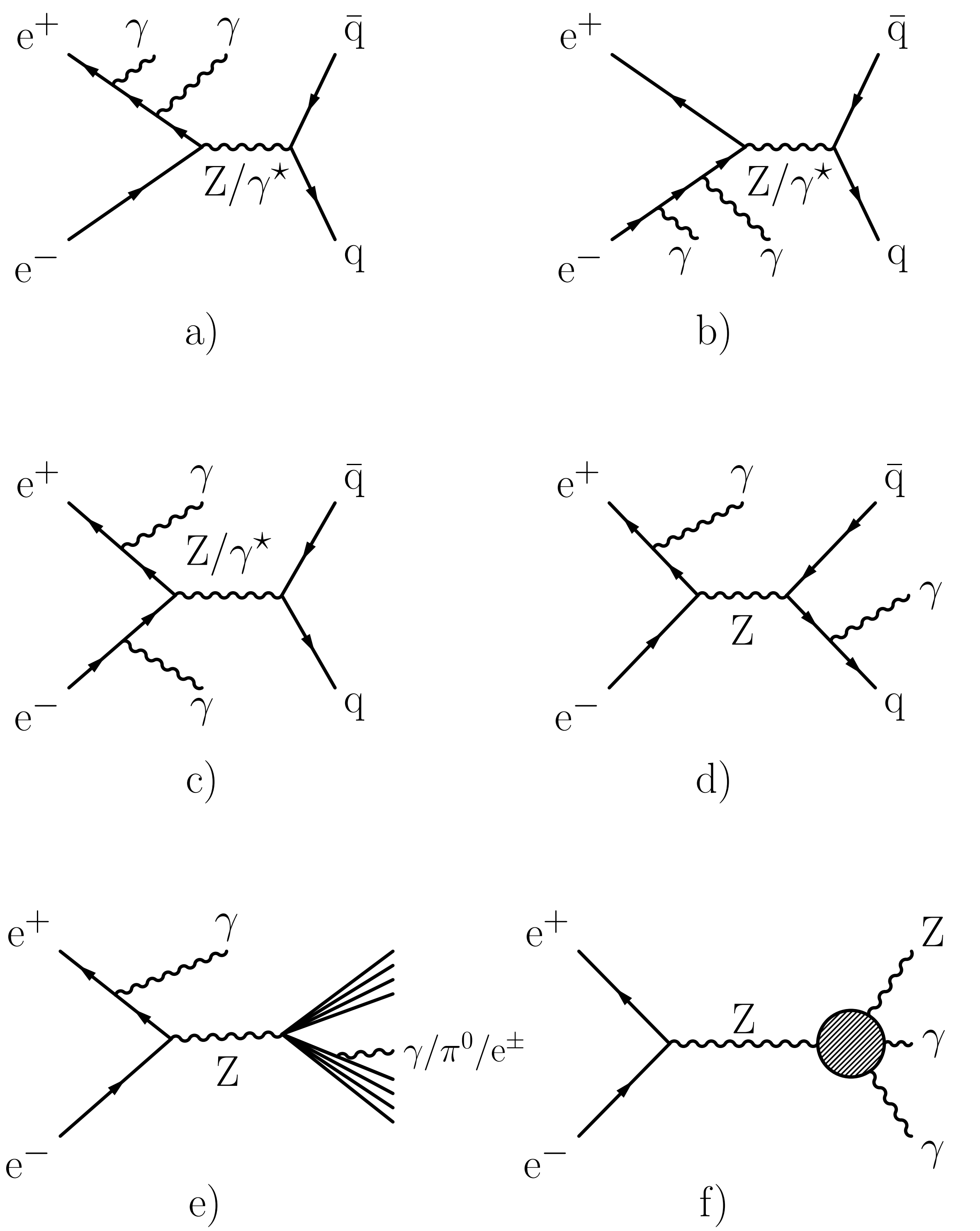

Figure 1: Representative diagrams of, a)–c), the Standard Model contribution to the $e^+e^- \rightarrow Z\gamma\gamma$ signal and the "non-resonant" background, d), the background from direct radiation of a photon from the quarks, e), the background from photons, misidentified electrons or unresolved π^0's originating from hadrons and, f), the anomalous QGC diagram.

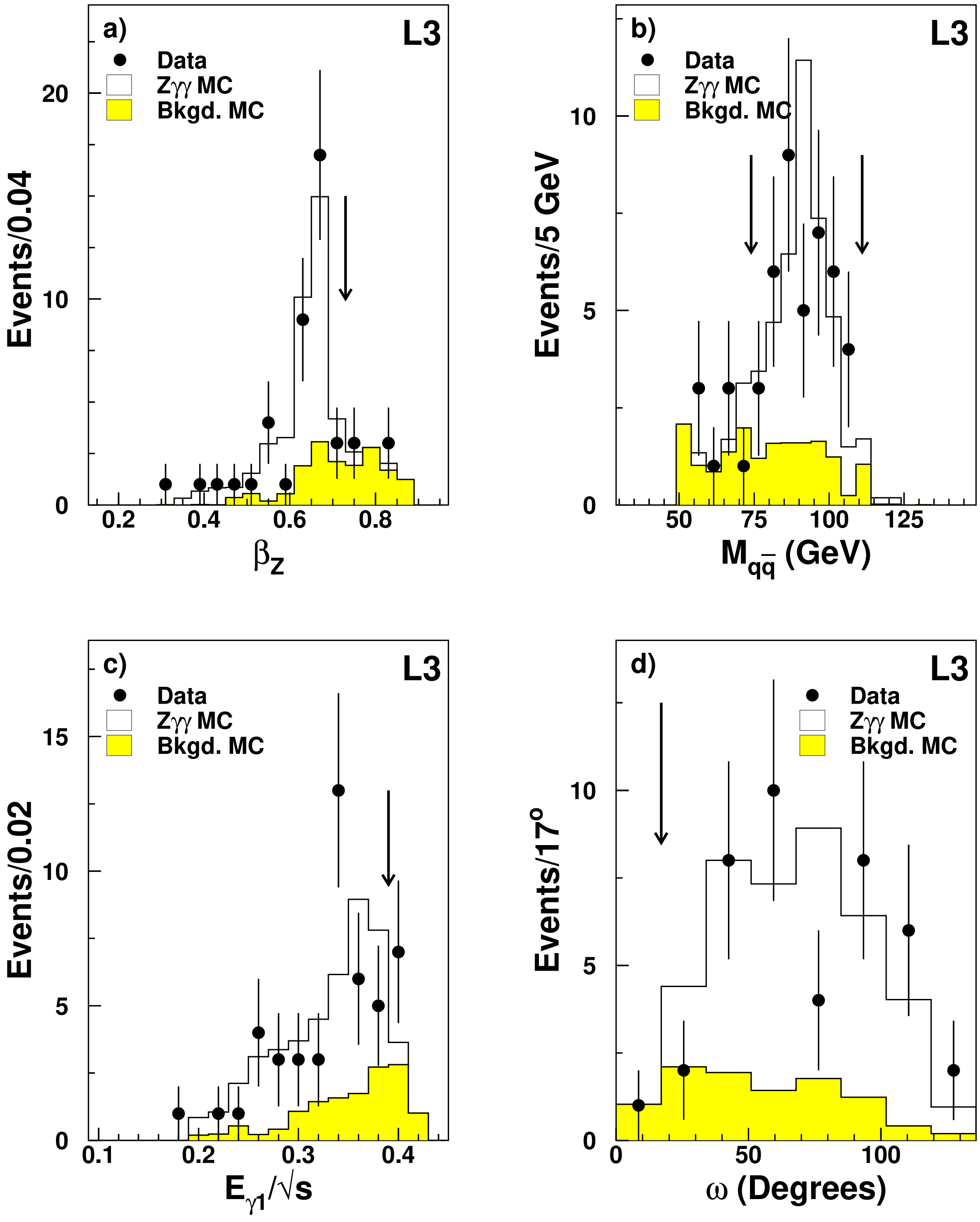

Figure 2: Distributions of, a), the relativistic velocity β_{Z} of the Z boson reconstructed from the measured photons, b), the invariant mass $M_{\mathrm{q\bar{q}}}$ of the hadronic system, c), the scaled energy $E_{\gamma1}/\sqrt{s}$ of the most energetic photon and, d), the angle ω between the least energetic photon and the nearest jet. Data, signal and background Monte Carlo samples are shown. Monte Carlo predictions are normalised to the integrated luminosity of the data. The arrows show the positions of the final selection cuts. In each plot, cuts on all other variables have been applied.

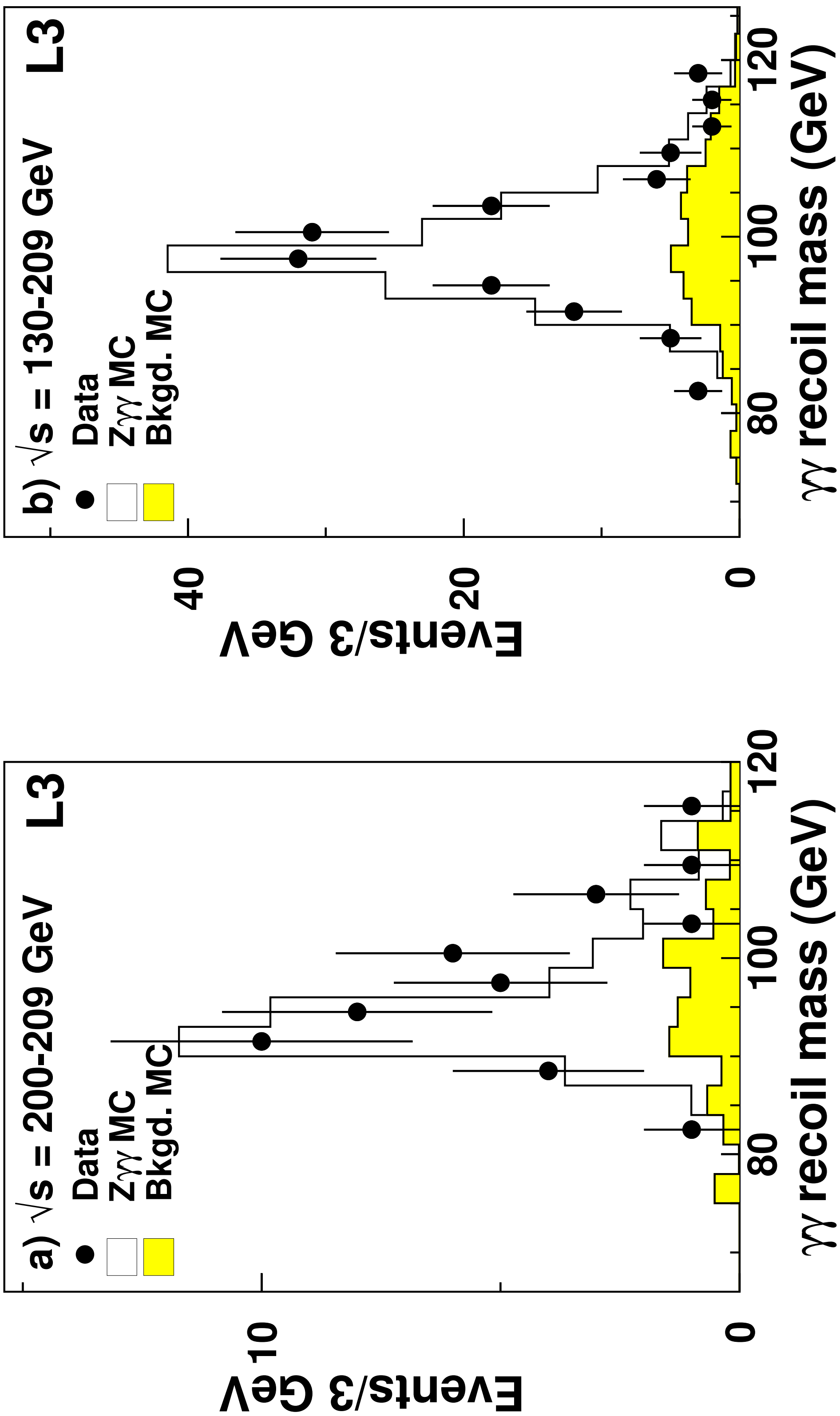

Figure 3: Mass recoiling from photon pairs in data, signal and background Monte Carlo for, a), the data sample analysed in this Letter and, b), the total sample collected above the Z resonance. Monte Carlo predictions are normalised to the integrated luminosity of the data.

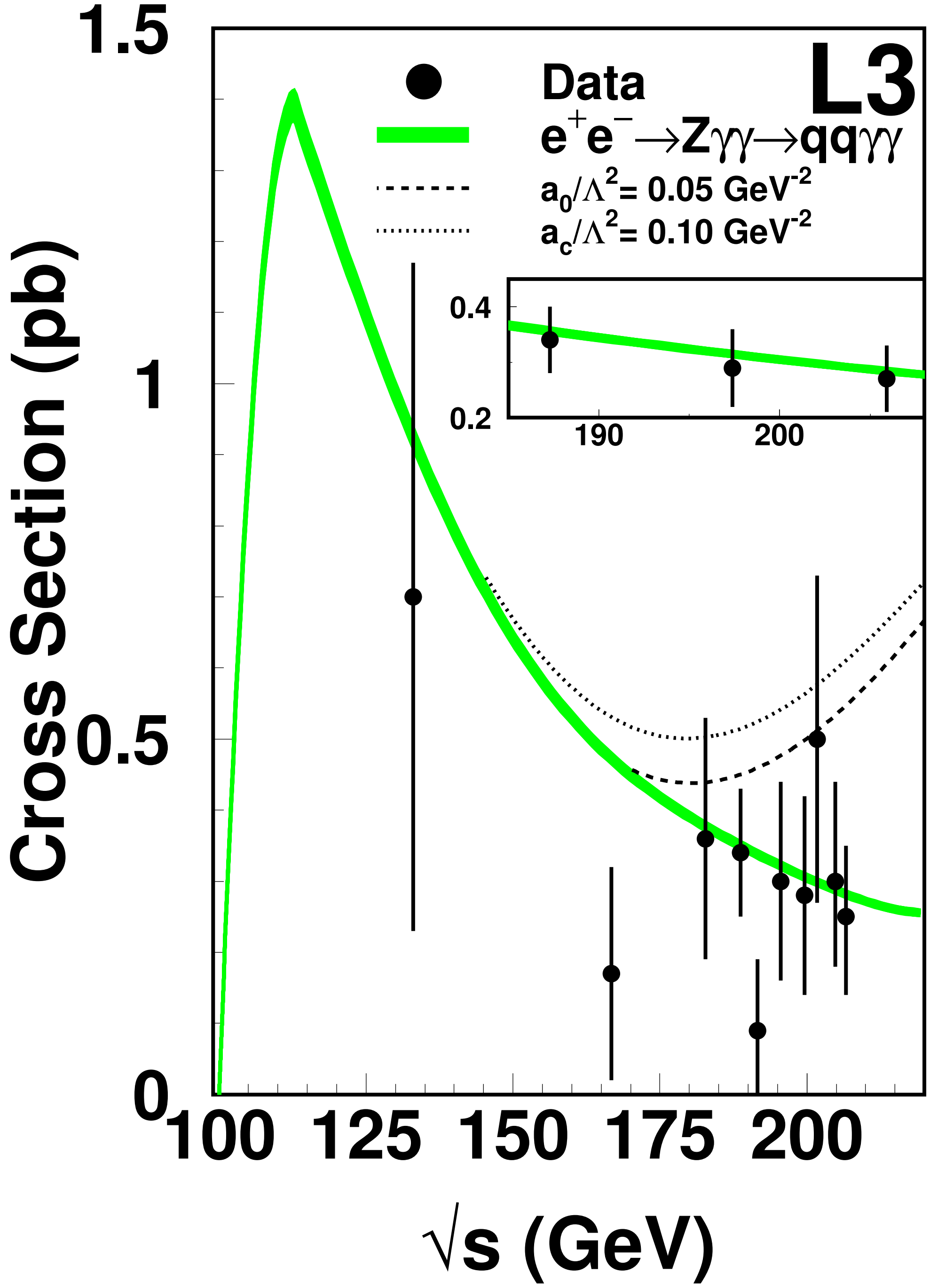

Figure 4: The cross section of the process $e^+e^- \rightarrow Z\gamma\gamma \rightarrow q\bar{q}\gamma\gamma$ as a function of $\sqrt{s}$. The signal is defined by the phase-space cuts of Equation (1). The width of the band corresponds to the statistical and theoretical uncertainties of the predictions of the KK2f Monte Carlo. Dashed and dotted lines represent anomalous QGC predictions for $a_0/\Lambda^2 = 0.05\ \mathrm{GeV}^{-2}$ and $a_c/\Lambda^2 = 0.10\ \mathrm{GeV}^{-2}$, respectively. The inset presents three combined samples: $231.6\mathrm{pb}^{-1}$ at $\sqrt{s} = 182.7 - 188.7$ GeV, $232.9\mathrm{pb}^{-1}$ at $\sqrt{s} = 191.6 - 201.7$ GeV and the data described in this Letter.

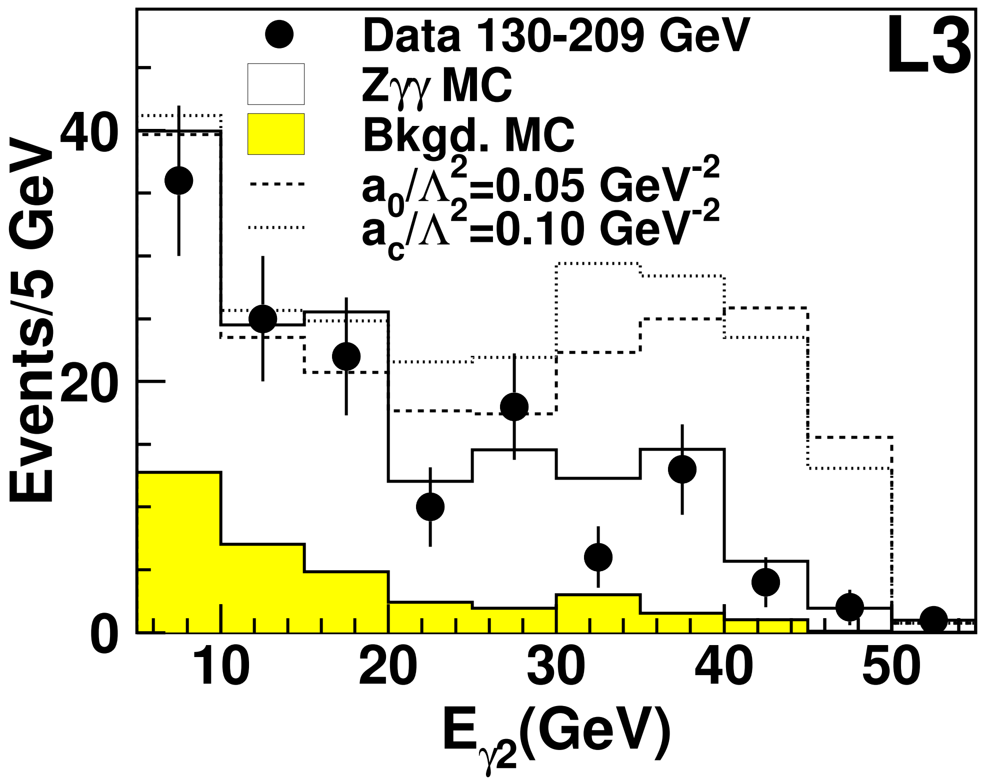

Figure 5: Energy spectrum of the least energetic photon in data, signal and background Monte Carlo. The full integrated luminosity at $\sqrt{s} = 130 - 209$ GeV is considered. Monte Carlo predictions are normalised to the integrated luminosity of the data. Examples of anomalous QGC predictions are also given.

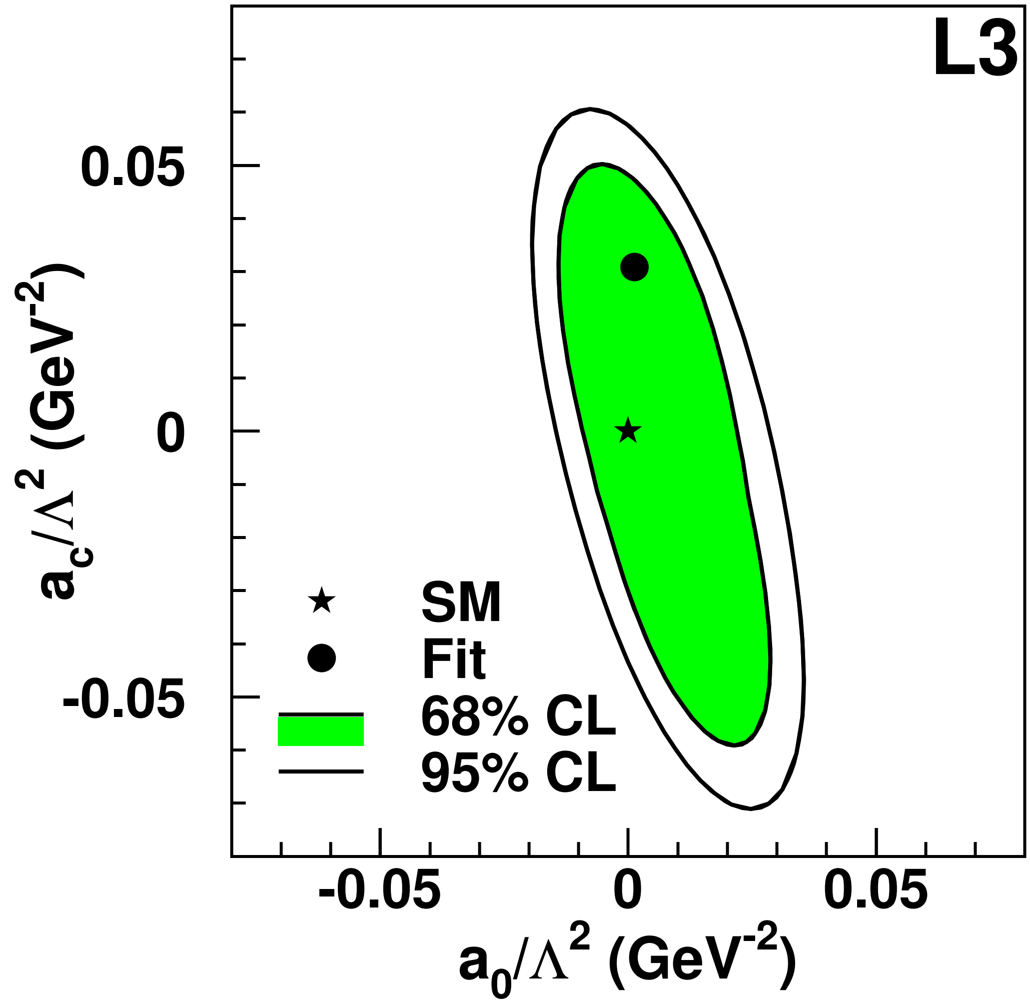

Figure 6: Two dimensional confidence level contours for the fitted QGC parameters a_0/Λ^2 and a_c/Λ^2. The fit result is shown together with the Standard Model (SM) predictions.